Published in final edited form as:
Gene Expr Patterns. 2013 December ; 13(8): . doi:10.1016/j.gep.2013.07.008.

Catalog of mRNA expression patterns for DNA methylating and demethylating genes in developing mouse lower urinary tract

Kimberly P. Keil[a], **Helene M. Altmann**[a], **Vatsal Mehta**[a], **Lisa L. Abler**[a], **Erik A. Elton**[a], and **Chad M. Vezina**[a,†]

[a]Department of Comparative Biosciences, University of Wisconsin-Madison, 1656 Linden Dr. Madison WI, 53706, USA.

Abstract

The mouse prostate develops from a component of the lower urinary tract (LUT) known as the urogenital sinus (UGS). This process requires androgens and signaling between mesenchyme and epithelium. Little is known about DNA methylation during prostate development, including which factors are expressed, whether their expression changes over time, and if DNA methylation contributes to androgen signaling or influences signaling between mesenchyme and epithelium. We used *in situ* hybridization to evaluate the spatial and temporal expression pattern of mRNAs which encode proteins responsible for establishing, maintaining or remodeling DNA methylation. These include DNA methyltrasferases, DNA deaminases, DNA glycosylases, base excision repair and mismatch repair pathway members. The mRNA expression patterns were compared between male and female LUT prior to prostatic bud formation (14.5 days post coitus (dpc)), during prostatic bud formation (17.5 dpc) and during prostatic branching morphogenesis (postnatal day (P) 5). We found dramatic changes in the patterns of these mRNAs over the course of prostate development and identified examples of sexually dimorphic mRNA expression. Future investigation into how DNA methylation patterns are established, maintained and remodeled during the course of embryonic prostatic bud formation may provide insight into prostate morphogenesis and disease.

Keywords

urogenital sinus; lower urinary tract; prostate; epigenetics; DNA methylation; DNA demethylation

1. Introduction

The fetal mouse prostate develops from the definitive urogenital sinus (UGS), a sub-compartment of the lower urinary tract (LUT) located between the bladder neck and caudal urethra. Prostate buds arise from UGS epithelium and require active androgen signaling in UGS mesenchyme (Cunha,1973, Hayashi et al., 1993, Lasnitzki and Mizuno,1980). In C57Bl/6J mice, prostate buds emerge and elongate between 16–18 days post coitus (dpc) (Lin et al., 2003, Vezina et al., 2008). The prostatic buds undergo branching morphogenesis

†Corresponding Author: cmvezina@wisc.edu. +1 608-890-3235.

Disclosure Statement: The authors have nothing to disclose.

which peaks around postnatal day (P) 5 (Sugimura et al., 1986). While many questions remain about the mechanisms of prostate development, emerging evidence suggests that DNA methylation may play a role (Anway et al., 2006, Dolinoy et al., 2007, 2006, Gupta, 2000, Ho et al., 2006, Sebag et al., 2011, Tang et al., 2012, Timms et al., 2005, Walker, 2011).

DNA methylation is an epigenetic event required for appropriate regulation of gene expression during embryonic development and throughout life (Laird and Jaenisch,1996). We are only beginning to understand how methylation marks are established and remodeled during development and how these events contribute to morphogenesis. Evidence of a role for DNA methylation in androgen-dependent prostate development has emerged from the field of toxicology. The developing prostate is exquisitely sensitive to endocrine disrupting chemicals. Embryonic exposure to the estrogenic endocrine disruptor bisphenol A (BPA) changes DNA methylation patterns and permanently reprograms prostate gene expression (Anway et al., 2006, Dolinoy et al., 2007, 2006, Gupta, 2000, Ho et al., 2006, Tang et al., 2012, Walker, 2011). Further, embryonic exposure to BPA and other estrogenic chemicals disturbs normal prostate budding morphogenesis and gene expression (Ho et al., 2006, Timms et al., 2005).

The prostate's requirement of active androgen signaling (Cunha,1973, Hayashi et al., 1993, Lasnitzki and Mizuno,1980) and its sensitivity to endocrine disrupting chemicals capable of altering DNA methylation raise the possibility that hormone action via DNA methylation may play a role in prostate morphogenesis. There are several reports of DNA methylation being affected by hormone action. Glucocorticoids influence DNA methylation patterns during brain development (Crudo et al., 2013). Gender differences exist in patterns of mouse left ventricle DNA methylation (Sebag et al 2011). These patterns are changed by gonadectomy and are associated with changes in gene expression, structure and function (Sebag et al 2011). In hormone responsive endometrium, DNA methyltransferase abundance changes during the menstrual cycle in synchrony with systemic hormone abundance (van Kaam et al., 2011, Vincent et al., 2011, Yamagata et al., 2009). Further, several genes display altered promoter methylation and mRNA abundance during the menstrual cycle, implantation and in endometriosis (Ding et al., 2012, Gao et al., 2012, Ghabreau et al., 2004, Wang et al., 2012, Yamagata et al., 2009, Zelenko et al., 2012). Changes in DNA methylation associated with polycystic ovary syndrome have been linked to androgens (Xu et al., 2011) and the androgen receptor (AR) interacts with and regulates epigenetic chromatin modifiers in adult prostate (Cai et al., 2011, Duan et al., 2012, Metzger et al., 2005, Wissmann et al., 2007). Together, these results suggest that hormone signaling can influence expression of DNA methylating proteins and model the DNA methylation landscape, raising the possibility that this could be a means of androgen action in the developing prostate. These results also raise the possibility that there are periods during which appropriate DNA methylation and demethylation are critical for normal prostate morphogenesis.

We cannot begin to sort out the role of DNA methylation in normal prostate development and in aberrant development in response to endocrine disrupting chemicals and other teratogens until we know which players are involved and where they are expressed. The purpose of this study is to characterize the mRNA expression pattern of genes involved in DNA methylation and demethylation during murine prostate development. We use *in situ* hybridization (ISH) to characterize these expression patterns in the male LUT prior to prostate development (14.5 dpc), during prostate bud formation (17.5 dpc) and during branching morphogenesis (P5) and in the female LUT which does not form appreciable prostatic ducts in the absence of androgens (Allgeier et al., 2010). Our results reveal mRNA pattern changes across developmental time and between males and females, revealing the

importance of characterizing these genes and their function during development. In future studies this characterization will enable us to test whether DNA methylation genes are regulated by steroid hormones, whether they mediate the actions of steroid hormones or whether they are needed for other reasons during prostate development.

2. Results

An ISH screen was conducted on 14.5 dpc, 17.5 dpc and P5 male and female 50-micron sagittal LUT sections as described previously (Abler et al., 2011a,b). The anatomical focus of this screen is the developing prostate and cranial aspect of the pelvic urethra from which it derives. The reason for analyzing mRNA expression in both sexes in late embryogenesis and early neonatal periods is because androgen signaling is more abundant in male than female LUT at these stages (Cooke et al.,1991, Takeda et al., 1991, 1987). We therefore seek to reveal mRNA patterns that possibly correspond with androgen signaling and prostate development in males during these stages. Age- and gender-matched samples were processed in the same tube and stained and imaged as a single experimental unit consisting of at least three samples per group. Immunohistochemistry (IHC) was used to label epithelium (anti-CDH1, red) and smooth muscle (anti-ACTA2, green) in each ISH-stained sample. Labeled epithelium and smooth muscle define boundaries between cell populations to facilitate high-resolution and consistent pattern mapping for each mRNA within the LUT subcompartments illustrated in Figure 1 and described previously (Abler et al., 2011b). The anatomical descriptors are based on Edinburgh Mouse Atlas Project and GUDMAP ontologies (Burger et al., 2004, Little et al., 2007, www.gudmap.org). In the results that follow, we only highlight noteworthy temporal, spatial or sex differences in mRNA expression within the prostate and cranial aspect of the pelvic urethra. Expression patterns for additional urethra-associated tissue compartments (bladder neck, Wolffian duct, ejaculatory duct, seminal vesicle, caudal Müllerian duct, upper vagina and lower vagina) are summarized in Supplemental Table 1 but are not discussed further.

2.1. DNA methyltransferase mRNAs are dynamic during embryonic and postnatal LUT development

DNA methyltransferase (*Dnmt*) enzymes catalyze methylation of the 5' carbon in cytosine. Three mammalian DNMTs are catalytically active: *Dnmt1, Dnmt3a* and *Dnmt3b* (Li et al., 1992, Okano et al.,1999). Although their patterns at each developmental stage are different, *Dnmt1, 3a* and *3b* mRNAs show some degree of overlap in how their urethral expression pattern changes during the period spanning 14.5 dpc to P5 (Fig.2). The trend is that *Dnmt* expression predominates in urethral mesenchyme during early development but gradually shifts to urethral epithelium and eventually prostatic bud tips in P5 male neonates (Fig. 2). The specific timing of this shift in expression is not the same for *Dnmt* family members. *Dnmt1* begins to localize to basal epithelium and prostatic buds by 17.5 dpc (Fig. 2B), while *Dnmt3a* and *Dnmt3b* localize to prostatic buds by P5 (Fig. 2I, O). Sex differences in *Dnmt1* staining are evident at P5 when *Dnmt1* is detected in a spotty pattern in periurethral mesenchyme (lamina propria and submucosa) of male but not female LUT sections (Fig. 2C, F). Sex differences for *Dnmt3a* and *Dnmt3b* are not apparent at the stages examined.

2.2. DNA demethylation pathway members are present in developing LUT before, during and after prostatic bud formation

DNA demethylation is less well understood than DNA methylation. It can occur passively by inhibition of *Dnmt1*, such that with each successive DNA synthesis event the level of methylation is reduced. DNA demethylation can also occur by an active process and several genes are capable of modifying and removing methyl groups from DNA. Active DNA

demethylation is thought to occur through events ranging from base modifications to base excision repair pathways.

Hydroxymethylation is a base modification known to occur throughout the genome and functions as a stable epigenetic mark and as an intermediate in the demethylation process (Guo et al., 2011, Ito et al., 2010, Tahiliani et al., 2009, Tan et al., 2012). Hydroxymethylation is catalyzed in part by members of the Ten-eleven translocation (Tet) family (*Tet1, Tet2* and *Tet3*) which convert 5-methylcytosine (5mC) to 5-hydroxymethylcytosine (5hmC) (Tahiliani et al., 2009).

The *Tets* are unlike the *Dnmts* in that there is no apparent trend within this family in how mRNA expression patterns change during LUT development from 14.5 dpc to P5. *Tet1* and *Tet2* predominate in urethral mesenchyme at 14.5 dpc and staining intensity therein increases from 14.5 dpc to 17.5 dpc (Fig. 3A – L). *Tet3* predominates in urethral epithelium at 14.5 dpc and staining intensity decreases therein from 14.5 dpc to P5 (Fig. 3M – O). The three *Tet* genes also differ in the stage and pattern in which they are first detected in urethral epithelium. *Tet1* staining is first visible in male urethral epithelium at P5 when it localizes to prostatic buds (Fig. 3C, solid arrowheads). *Tet2* staining is detectable in urethral epithelium at 14.5 dpc and thereafter is restricted to intermediate and superficial urethral epithelium and is not apparent in prostatic buds (Fig. 3H; inset, solid arrowheads). *Tet3* staining is present in urethral and prostatic bud epithelium at 14.5 dpc, 17.5 dpc and P5 (Fig. 3M–O, solid arrowheads).

There are some noteworthy sex differences in *Tet* staining patterns within the LUT. At 17.5 dpc *Tet1* is not detected in male epithelium but is present in a spotted pattern in female urethral epithelium (Fig. 3B, E; insets). At 17.5 dpc *Tet2* staining is weaker throughout urethral epithelium in male compared to female LUT (Fig. 3 H, K; insets). A sex difference for *Tet3* staining is observed at 17.5 dpc when light staining exists in male but not female urethral smooth muscle mesenchyme (Fig. 3N, Q).

Another proposed mechanism of DNA demethylation is through cytidine deamination, which converts 5mC to thymine to create a T:G mismatch which activates DNA repair pathways (Bhutani et al., 2010, Muramatsu et al., 2000, Morgan et al., 2004, Popp et al., 2010, Rai et al., 2008). Cytidine deamination is mediated by activation induced cytidine deaminase (*Aicda*, or *Aid*) and apolipoprotein B mRNA editing enzyme, catalytic polypeptide 1–3 (*Apobec1, 2* and *3*), which are collectively referred to as AID/APOBEC family members.

AID/APOBEC family members exhibit unique spatiotemporal mRNA expression patterns in the mouse LUT. *Aicda* mRNA staining is detected in 14.5 dpc fetal urethral mesenchyme and epithelium where it gradually decreases until at least P5 (Fig. 4A – C). *Apobec1* mRNA staining was absent from urethral mesenchyme and epithelium of the male at the time points examined (Fig. 4G – I). *Apobec2* staining in urethral and prostatic bud epithelium persists from 14.5 dpc to P5 while staining in urethral mesenchyme is restricted to smooth muscle by 17.5 dpc (Fig. 4M – O). Weak *Apobec3* staining is present in urethral mesenchyme and epithelium at 14.5 dpc which gradually increases until at least 17.5 dpc before staining is again reduced and no longer detected in urethral mesenchyme by P5 (Fig. 4S – U). There are no noteworthy sex differences in AID/APOBEC staining within the LUT at 14.5 dpc, 17.5 dpc or P5.

As part of DNA damage repair, DNA glycosylases remove damaged DNA bases which are then repaired through the base excision repair pathway (Jost et al., 1995, Jost, 1993). There are several DNA glycosylases including: thymine DNA glycosylase (*Tdg*), uracil DNA glycosylase (*Ung*), single-strand selective monofunctional uracil DNA glycosylase (*Smug1*)

and methyl-CpG binding domain protein 4 (*Mbd4*) that have been identified to play specific roles in DNA demethylation. *Tdg* glycosylase activity is necessary for murine development and establishing proper DNA methylation patterns (Cortellino et al., 2011). While there is evidence that *Tdg* and *Mbd4* can recognize and bind 5mC:G *in vitro* (Zhu, 2009, Zhu et al., 2000a, b), all of the DNA glycosylases are capable of participating in DNA demethylation by recognizing and removing T:G or U:G mismatches generated from the AID/APOBEC family or from deamination of a *Tet* mediated 5hmC (Cortellino et al., 2011, Guo et al., 2011a, b).

The DNA glycosylases predominate in epithelium at 14.5 dpc and 17.5 dpc but their expression subsequently dissipates by P5 (Fig. 5, Fig. 6A – F). Surprisingly, these mRNAs also differ in their location within the epithelium prior to P5. *Tdg* is found in all urethral epithelium layers including prostatic buds (Fig. 5A–C, solid arrowheads), *Ung* epithelial staining becomes restricted to prostatic bud epithelium by 17.5 dpc (Fig. 5G – I), *Smug1* epithelial staining is localized to intermediate and superficial epithelium (Fig. 5M–O; insets) and *Mbd4* staining is found in all epithelium including prostatic buds until at least 17.5 dpc (Fig. 6A – C). A few DNA glycosylases also display light mesenchymal staining which also dissipates by P5 (Fig. 5, Fig. 6A – F). *Tdg* and *Smug1* staining is detected in urethral smooth muscle mesenchyme at 17.5 dpc while *Mbd4* staining in urethral mesenchyme is uniquely increased until at least 17.5 dpc before it is no longer detected at P5 (Fig. 6A – C). Differences between sexes are observed for *Tdg* at 17.5 dpc and for *Ung* and *Mbd4* at P5. At 17.5 dpc *Tdg* staining is present in male but absent in female urethral mesenchyme (Fig. 5B, E). At P5 *Ung* staining is absent from the male but present in female urethral epithelium (Fig. 5I, L). Also at P5, *Mbd4* staining is present in male but not female urethral epithelium (Fig. 6C, F).

Mbd4 is the only MBD family member with glycosylase activity but *Mbd2* may also contribute to DNA demethylation. *Mbd2* is reported to have demethylase activity, though this is controversial and doesn't exclude the possibility that *Mbd2* acts in concert with other factors in the demethylation process (Bhattacharya et al., 1999, Hamm et al., 2008, McGowan et al., 1997, Ng et al., 1999). Unlike *Mbd4, Mbd2* predominates in epithelium especially within intermediate and superficial urethral epithelial layers (Fig. 6H; insets). By P5 *Mbd2* staining in urethral epithelium is diminished and only detected in tips of prostatic buds (Fig. 6I, solid arrowheads) and a small portion of the pelvic urethra. A similar dissipation of *Mbd2* staining during the 14.5 dpc to P5 period is observed for female urethral epithelium (Fig. 6J – L) and there are no apparent sex differences at the time points examined.

Mismatches generated by AID/APOBEC family members are also recognized by the DNA mismatch repair pathway. The DNA mismatch repair proteins excise and replace an entire region surrounding a mismatch; therefore one CpG mismatch site could lead to demethylation of surrounding sites (Franchini et al., 2012, Modrich, 2006). MutS homolog 2 (*Msh2*), is the common subunit of the MutS alpha and MutS beta heterodimer which recognizes and binds mismatches in DNA (Acharya et al., 1996, Iaccarino et al., 1998, Gradia et al., 1999, Su et al., 1986, de Wind et al., 2005, Varlet et al., 1994, Prolla et al 1994, Reenan et al., 1992, Modrich et al 1991). Binding of the MSH2 complex to DNA mismatches initiates the repair process by recruiting the MutL alpha complex consisting of MutL homolog 1 (*Mlh1*) and postmeiotic segregation increased 2 (*Pms2*) which possess endonuclease activity (Kadyrov et al., 2006, Prolla et al 1994). *Msh2, Mlh1* and *Pms2* are also often decreased in prostate cancer (Barrow et al., 2013, Chen et al., 2003, Soni et al., 2011, Wagner et al., 2010).

The mismatch repair pathway members *Msh2, Mlh1* and *Pms2* predominate in epithelium at 14.5 dpc, 17.5 dpc and P5 but their expression patterns in urethral mesenchyme vary (Fig. 7A – R). While *Msh2* is not detected in urethral mesenchyme at the time points examined (Fig. 7A – F), *Mlh1* is detected in urethral mesenchyme (Fig. 7G – L). *Mlh1* staining in peri-prostatic mesenchyme diminishes from 17.5 dpc to P5 (Fig. 7G – L). *Pms2* staining is present in urethral mesenchyme at 14.5 dpc but dissipates by P5 (Fig. 7M – R). No apparent sex differences are observed at the time points examined.

Chromatin modifiers also participate in the DNA damage response. Chromodomain helicase DNA binding protein 2 (*Chd2*), a chromatin remodeling gene, is required for repair of damaged DNA (Nagarajan et al., 2009, Rajagopalan et al., 2012) and is necessary for normal kidney development and function (Marfella et al., 2008, 2006). *Chd2* staining is detected in mesenchyme and epithelium at 14.5 dpc (Fig. 7S). Mesenchymal staining is reduced after 14.5 dpc and epithelial staining is strongest in intermediate urethral epithelium (Fig. 7T; inset). A sex difference for *Chd2* staining exists at 17.5 dpc where basal urethral epithelial staining is less apparent in male compared to female urethra (Fig. 7T, W; insets).

3. Discussion

The focus of this study was to identify spatial and temporal changes in the mRNA staining patterns of genes implicated in adding, maintaining or removing DNA methylation marks and to determine whether their expression patterns are different in male and female LUT. Whether corresponding proteins are present, active or lead to biologically significant changes in DNA methylation was not determined and is beyond the scope of this study. Though ISH has some limitations, including the inability to quantify transcript level, ISH is uniquely suited for determining when and where genes involved in DNA methylation are expressed in the developing prostate. We have discussed previously measures taken to ensure the sensitivity and specificity of our ISH method in terms of riboprobe design, sample processing and validation (Abler et al., 2011a,b, Keil et al., 2012, Mehta et al., 2011). Additionally, all gender-and age-matched samples were run in the same tube during ISH and color development.

We describe for the first time a comprehensive mRNA expression atlas for genes involved or suspected to be involved in DNA methylation and demethylation over the course of early mouse prostate development. These gene products are hypothesized to be involved in remodeling the epigenome by establishing, erasing or maintaining methylation so the proper DNA methylation patterns exist for normal development, cellular plasticity and differentiation. One of the interesting findings was that the LUT cell populations expressing these mRNAs changed during the course of early prostate development in males. While the focus of this study was DNA methylation, the temporal shift in mRNA expression we observed in several genes is consistent with what others have observed for epigenetic chromatin modifiers. Enhancer of zeste homolog 2 (*Ezh2*), a subunit of the polycomb repressor complex 2 involved in chromatin remodeling (H3K27 methylation), changes temporally during mouse UGS development, with embryonic epithelial and mesenchymal expression that becomes restricted to luminal epithelium by P10 (Duan et al., 2012). How these changes in DNA methylation and chromatin remodeling gene expression patterns relate to prostate morphogenesis and prostate cell differentiation remains to be determined. Our results provide information which will enable future studies to specifically target these genes for deletion or assess their activity in the appropriate tissue and during the appropriate time to see whether they participate in prostate development.

A change in mRNA staining pattern commonly observed over the course of prostate development is urethral mesenchymal expression as early as 14.5 dpc which becomes less

predominant or shifts to epithelium by P5. The significance of this change in staining pattern is that it occurs during the critical window when androgens are eliciting their actions in urethral mesenchyme to direct prostate development (14.5–17.5 dpc) (Lasnitzki and Mizuno 1977). Future studies will be necessary to determine if these genes play a role in the instructive potential of urethral mesenchyme (Cunha, 2008, Cunha et al., 1983). These temporal changes may also be significant in understanding how developmental pathways are inappropriately reawakened during disease. A recent study of the chromatin remodeling gene high mobility group AT-hook 2 (*Hmga2*) found that it is also more abundant in embryonic urethral mesenchyme compared to adult stroma (Zong et al., 2012). When *Hmga2* is overexpressed in immortalized prostate mesenchymal cells and these cells are combined with non-tumorigenic adult mouse prostate epithelium and grafted into a host mouse, the resultant graft forms high-grade prostate intraepithelial neoplasia (Zong et al., 2012), a hypothesized precursor lesion to prostate cancer (Bostwick and Qian 2004, Lee et al. 2010). This result is evidence that inappropriate epigenetic alterations in prostate stroma can change the behavior of prostate cells associated with it (Zong et al., 2012). Together these results highlight the need for additional studies into how DNA methylation patterns are established, maintained and remodeled during the course of embryonic prostatic bud formation and specifically if and how the actions of other DNA methylation modifiers in prostate stroma influence prostate epithelial morphogenesis, differentiation and proliferation.

The androgen receptor is capable of interacting with or regulating the epigenome via chromatin modifiers including lysine specific demethylase 1 (*Lsd1* or *Kdm1a*), enhancer of zeste homolog 2 (*Ezh2*) and mixed lineage leukemia 1 (*MII1*) (Cai et al., 2011, Duan et al., 2012, Metzger et al., 2005, Wissmann et al., 2007). Whether the AR is involved with other epigenetic modifications such as DNA methylation and whether this occurs during prostate development has never been determined. *Dnmt* expression changes during the human female menstrual cycle and *Dnmt3a* and *3b* are regulated by female sex hormones *in vitro* (van Kaam et al., 2011, Yamagata et al., 2009). Though we identified a few mRNAs which were noticeably different in pattern or abundance between male and female LUT, none of these displayed a pattern similar to the known androgen responsive genes steroid 5 alpha reductase 2 (*Srd5a2*) and WNT inhibitory factor 1 (*Wif1*) (Abler et al., 2011b, Keil et al., 2012, Matsui et al., 2002). While we did not look into the regulation of these genes by sex hormones, these observations suggest that these genes are likely not regulated by androgens in the male LUT, at least not directly or in the same manner as the androgen responsive genes mentioned above. This does not preclude the possibility that some DNA methylation modifying genes are post-transcriptionally modified or involved with AR signaling in some other capacity. Whether these genes act upstream, in concert with or independently of androgen signaling remains to be determined. Future investigation into the mechanism controlling these genes during prostate development and how their downstream actions direct prostatic bud formation will be useful tools in prostate research.

4. Experimental Procedures

4.1. Animals

Wild type C57BL/6J mice (Jackson Laboratory, Bar Harbor, ME) were maintained on a 12 hr light and dark cycle at 25±5°C and 20–50% humidity. Feed (Diet 2019 for males and 7002 for females, Harlan Teklad, Madison, WI) and water were available *ad libitum*. All procedures were approved by the University of Wisconsin Animal Care and Use Committee and conducted in accordance with the NIH Guide for Care and Use of Laboratory Animals. To obtain timed pregnant dams, female mice were paired overnight with males and the next morning was considered 0.5 dpc. Dams were euthanized by CO2 asphyxiation and fetuses were maintained in phosphate-buffered saline prior to dissection.

4.2. *In Situ* Hybridization (ISH)

Tissue collection, storage, sectioning and ISH were conducted as described previously (Abler et al., 2011a,b). Primer sequences used to generate probe templates are provided in Table 1. We used the Primer Blast Program (Ye et al., 2012) to ensure specificity of PCR primers for the target sequence. We selected primer sequences that uniquely matched the target sequence and no other sequence in the mouse reference genome. We used the MegaBLAST program (Zhang et al., 2000) to ensure specificity of the riboprobe sequence. The riboprobe sequence was considered specific for its target when, using an EXPECT threshold of 0.01 and a word size of 128, it did not align with other members of the mouse RefSeq RNA database. A positive control gene (uroplakin 1b) as well as a no probe negative control was used to ensure run quality. The run was considered high quality when: 1) uroplakin 1b staining emerged within the expected window of staining development time (1–3 hours) and was uniquely localized to intermediate and superficial urothelium and 2) when no staining was detected in no probe control tissues with up to 100 hours of development time. The staining pattern for each riboprobe was assessed in at least two LUT sections/mouse and at least three litter-independent LUTs. Age- and gender-matched samples were processed together in a single tube for ISH and color development to allow for qualitative comparisons among biological replicates and between male and female for each stage examined. All stage- and gender-differences in staining patterns reported in this manuscript were observed across all three litter independent samples per group. Additional images of some ISH-stained LUT sections are available at www.gudmap.org.

4.3. Immunohistochemistry (IHC)

IHC was conducted on ISH-stained sections as described previously (Abler et al., 2011b). Primary antibodies used were: rabbit anti-CDH1 (1:300, Cell Signaling Technologies, Beverly, MA) and mouse anti-ACTA2 (1:300, Leica Microsystems, Bannockburn, IL). Secondary antibodies used were: Dylight 488-conjugated goat anti-mouse IgG (1:500) and Dylight 546-conjucated goat anti-rabbit IgG (1:500) (Jackson Immunoresearch, West Grove, PA). Sections were mounted in anti-fade media (phosphate-buffered saline containing 80% glycerol and 0.2% n-propyl gallate). Sections were imaged on an Eclipse E600 compound microscope (Nikon Instruments Inc., Melville, NY). Brightfield (ISH, purple) and fluorescent (red, green) images were merged using NIS elements imaging software (Nikon Instruments Inc). No modifications were made to brightfield ISH images. Fluorescent channels were adjusted to optimize brightness and contrast.

Supplementary Material

Refer to Web version on PubMed Central for supplementary material.

Acknowledgments

This work was supported by National Institutes of Health Grants DK083425, DK070219 and DK096074 (to C.M.V), and National Science Foundation Grant DGE-0718123 (to K.P.K).

Abbreviations

LUT	lower urinary tract
UGS	urogenital sinus
dpc	days post coitus
P	postnatal day

AR	androgen receptor
ISH	*in situ* hybridization
IHC	immunohistochemistry

References

Abler LL, Mehta V, Keil KP, Joshi PS, Flucus C, Hardin HA, Schmitz CT, Vezina CM. A high throughput in situ hybridization method to characterize mrna expression patterns in the fetal mouse lower urogenital tract. J Vis Exp. 2011a; 54:pii2912.

Abler LL, Keil KP, Mehta V, Joshi PS, Schmitz CT, Vezina CM. A high-resolution molecular atlas of the fetal mouse lower urogenital tract. Dev. Dyn. 2011b; 240:2364–2377. [PubMed: 21905163]

Allgeier SH, Lin T, Moore RW, Vezina CM, Abler LL, Peterson RE. Androgenic regulation of ventral epithelial bud number and pattern in mouse urogenital sinus. Dev. Dyn. 2010; 239:373–385. [PubMed: 19941349]

Anway MD, Leathers C, Skinner MK. Endocrine disruptor vinclozolin induced epigenetic transgenerational adult-onset disease. Endocrinol. 2006; 147:5515–5523.

Acharya S, Wilson T, Gradia S, Kane MF, Guerrette S, Marsischky GT, Kolodner R, Fishel R. hMSH2 forms specific mispair-binding complexes with hMSH3 and hMSH6. ProcNatl Acad Sci USA. 1996; 93:13629–13634.

Barrow PJ, Ingham S, O'Hara C, Green K, McIntyre I, Lalloo F, Hill J, Evans DG. The spectrum of urological malignancy in Lynch syndrome. Fam Cancer. 2013; 12:57–63. [PubMed: 23054215]

Bhattacharya SK, Ramchandani S, Cervoni N, Szyf M. A mammalian protein with specific demethylase activity for mcpg dna. Nature. 1999; 397:579–583. [PubMed: 10050851]

Bhutani N, Brady JJ, Damian M, Sacco A, Corbel SY, Blau HM. Reprogramming towards pluripotency requires aid-dependent dna demethylation. Nature. 2010; 463:1042–1047. [PubMed: 20027182]

Bostwick DG, Qian J. High-grade prostatic intraepithelial neoplasia. Modern Pathol. 2004; 17:360–379.

Burger A, Davidson D, Baldock R. Formalization of mouse embryo anatomy. Bioinformatics. 2004; 20:259–267. [PubMed: 14734318]

Cai C, He HH, Chen S, Coleman I, Wang H, Fang Z, Chen S, Nelson PS, Liu XS, Brown M, Balk SP. Androgen receptor gene expression in prostate cancer is directly suppressed by the androgen receptor through recruitment of lysine-specific demethylase 1. Cancer Cell. 2011; 20:457–471. [PubMed: 22014572]

Chen Y, Wang J, Fraig MM, Henderson K, Bissada NK, Watson DK, Schweinfest CW. Alterations in PMS2, MSH2, and MLH1 expression in human prostate cancer. Int J Oncol. 2003; 22:1033–1043. [PubMed: 12684669]

Cooke PS, Young P, Cunha GR. Androgen receptor expression in developing male reproductive organs. Endocrinol. 1991; 128:2867–2873.

Cortellino S, Xu J, Sannai M, Moore R, Caretti E, Cigliano A, Le Coz M, Devarajan K, Wessels A, Soprano D, Abramowitz LK, Bartolomei MS, Rambow F, Bassi MR, Bruno T, Fanciulli M, Renner C, Klein-Szanto AJ, Matsumoto Y, Kobi D, Davidson I, Alberti C, Larue L, Bellacosa A. Thymine dna glycosylase is essential for active dna demethylation by linked deamination-base excision repair. Cell. 2011; 146:67–79. [PubMed: 21722948]

Crudo A, Suderman M, Moisiadis VG, Petropoulos S, Kostaki A, Hallett M, Szyf M, Matthews SG. Glucocorticoid programming of the fetal male hippocampal epigenome. Endocrinol. 2013; 154:1168–1180.

Cunha GR. The role of androgens in the epithelio-mesenchymal interactions involved in prostatic morphogenesis in embryonic mice. Anat. Rec. 1973; 175:87–96. [PubMed: 4734188]

Cunha GR. Mesenchymal-epithelial interactions: past, present, and future. Differentiation. 2008; 76:578–586. [PubMed: 18557761]

Cunha GR, Fujii H, Neubauer BL, Shannon JM, Sawyer L, Reese BA. Epithelial-mesenchymal interactions in prostatic development. i. morphological observations of prostatic induction by urogenital sinus mesenchyme in epithelium of the adult rodent urinary bladder. J. Cell Biol. 1983; 96:1662–1670. [PubMed: 6853597]

de Wind N, Dekker M, Berns A, Radman M, te Riele H. Inactivation of the mouse Msh2 gene results in mismatch repair deficiency, methylation tolerance, hyperrecombination, and predisposition to cancer. Cell. 1995; 82:321–330. [PubMed: 7628020]

Ding Y, Long C, Liu X, Chen X, Guo L, Xia Y, He J, Wang Y. 5-aza-2'-deoxycytidine leads to reduced embryo implantation and reduced expression of dna methyltransferases and essential endometrial genes. PLoS One. 2012; 7:e45364. [PubMed: 23028963]

Dolinoy DC, Weidman JR, Jirtle RL. Epigenetic gene regulation: linking early developmental environment to adult disease. Reprod. Toxicol. 2007; 23:297–307. [PubMed: 17046196]

Dolinoy DC, Weidman JR, Waterland RA, Jirtle RL. Maternal genistein alters coat color and protects avy mouse offspring from obesity by modifying the fetal epigenome. Environ. Health Perspect. 2006; 114:567–572. [PubMed: 16581547]

Duan Z, Zou JX, Yang P, Wang Y, Borowsky AD, Gao AC, Chen H. Developmental and androgenic regulation of chromatin regulators ezh2 and ancca/atad2 in the prostate via mll histone methylase complex. Prostate. 2012

Franchini D, Schmitz K, Petersen-Mahrt SK. 5-methylcytosine dna demethylation: more than losing a methyl group. Annu. Rev. Genet. 2012; 46:419–441. [PubMed: 22974304]

Gao F, Ma X, Rusie A, Hemingway J, Ostmann AB, Chung D, Das SK. Epigenetic changes through dna methylation contribute to uterine stromal cell decidualization. Endocrinol. 2012; 153:6078–6090.

Ghabreau L, Roux JP, Niveleau A, Fontanière B, Mahe C, Mokni M, Frappart L. Correlation between the dna global methylation status and progesterone receptor expression in normal endometrium, endometrioid adenocarcinoma and precursors. Virchows Arch. 2004; 445:129–134. [PubMed: 15221375]

Gradia S, Subramanian D, Wilson T, Acharya S, Makhov A, Griffith J, Fishel R. hMSH2-hMSH6 forms a hydrolysis-independent sliding clamp on mismatched DNA. Mol Cell. 1999; 3:255–261. [PubMed: 10078208]

Guo JU, Su Y, Zhong C, Ming G, Song H. Hydroxylation of 5-methylcytosine by tet1 promotes active dna demethylation in the adult brain. Cell. 2011a; 145:423–434. [PubMed: 21496894]

Guo JU, Su Y, Zhong C, Ming G, Song H. Emerging roles of tet proteins and 5-hydroxymethylcytosines in active dna demethylation and beyond. Cell Cycle. 2011b; 10:2662–2668. [PubMed: 21811096]

Gupta C. Reproductive malformation of the male offspring following maternal exposure to estrogenic chemicals. Proc. Soc. Exp. Biol. Med. 2000; 224:61–68. [PubMed: 10806412]

Hamm S, Just G, Lacoste N, Moitessier N, Szyf M, Mamer O. On the mechanism of demethylation of 5-methylcytosine in dna. Bioorg. Med. Chem. Lett. 2008; 18:1046–1049. [PubMed: 18162397]

Hayashi N, Cunha GR, Parker M. Permissive and instructive induction of adult rodent prostatic epithelium by heterotypic urogenital sinus mesenchyme. Epithelial Cell Biol. 1993; 2:66–78. [PubMed: 8353595]

Ho S, Tang W, Belmonte de Frausto J, Prins GS. Developmental exposure to estradiol and bisphenol a increases susceptibility to prostate carcinogenesis and epigenetically regulates phosphodiesterase type 4 variant 4. Cancer Res. 2006; 66:5624–5632. [PubMed: 16740699]

Iaccarino I, Marra G, Palombo F, Jiricny J. hMSH2 and hMSH6 play distinct roles in mismatch binding and contribute differently to the ATPase activity of hMutSalpha. EMBO J. 1998; 17:2677–2686. [PubMed: 9564049]

Ito S, D'Alessio AC, Taranova OV, Hong K, Sowers LC, Zhang Y. Role of tet proteins in 5mc to 5hmc conversion, es-cell self-renewal and inner cell mass specification. Nature. 2010; 466:1129–1133. [PubMed: 20639862]

Jost JP. Nuclear extracts of chicken embryos promote an active demethylation of dna by excision repair of 5-methyldeoxycytidine. Proc. Natl. Acad. Sci. U.S.A. 1993; 90:4684–4688. [PubMed: 8506318]

Jost JP, Siegmann M, Sun L, Leung R. Mechanisms of dna demethylation in chicken embryos. purification and properties of a 5-methylcytosine-dna glycosylase. J. Biol. Chem. 1995; 270:9734–9739. [PubMed: 7730351]

Kadyrov FA, Dzantiev L, Constantin N, Modrich P. Endonucleolytic function of MutLalpha in human mismatch repair. Cell. 2006; 126:297–308. [PubMed: 16873062]

Keil KP, Mehta V, Branam AM, Abler LL, Buresh-Stiemke RA, Joshi PS, Schmitz CT, Marker PC, Vezina CM. Wnt inhibitory factor 1 (wif1) is regulated by androgens and enhances androgen-dependent prostate development. Endocrinol. 2012; 153:6091–6103.

Laird PW, Jaenisch R. The role of dna methylation in cancer genetic and epigenetics. Annu. Rev. Genet. 1996; 30:441–464. [PubMed: 8982461]

Lasnitzki I, Mizuno T. Prostatic induction: interaction of epithelium and mesenchyme from normal wild-type mice and androgen-insensitive mice with testicular feminization. J. Endocrinol. 1980; 85:423–428. [PubMed: 7411008]

Lasnitzki I, Mizuno T. Induction of the rat prostate gland by androgens in organ culture. J. Endocr. 1977; 74:47–55. [PubMed: 874417]

Lee MC, Moussa AS, Yu C, Kattan MW, Magi-Galluzzi C, Jones SJ. Multifocal high grade prostatic intraepithelial neoplasia is a risk factor for subsequent prostate cancer. J. Urol. 2010; 184:1958–1962. [PubMed: 20846692]

Li E, Bestor TH, Jaenisch R. Targeted mutation of the dna methyltransferase gene results in embryonic lethality. Cell. 1992; 69:915–926. [PubMed: 1606615]

Lin T, Rasmussen NT, Moore RW, Albrecht RM, Peterson RE. Region-specific inhibition of prostatic epithelial bud formation in the urogenital sinus of c57bl/6 mice exposed in utero to 2,3,7,8-tetrachlorodibenzo-p-dioxin. Toxicol. Sci. 2003; 76:171–181. [PubMed: 12944588]

Little MH, Brennan J, Georgas K, Davies JA, Davidson DR, Baldock RA, Beverdam A, Bertram JF, Capel B, Chiu HS, Clements D, Cullen-McEwen L, Fleming J, Gilbert T, Herzlinger D, Houghton D, Kaufman MH, Kleymenova E, Koopman PA, Lewis AG, McMahon AP, Mendelsohn CL, Mitchell EK, Rumballe BA, Sweeney DE, Valerius MT, Yamada G, Yang Y, Yu J. A high-resolution anatomical ontology of the developing murine genitourinary tract. Gene Expr. Patterns. 2007; 7:680–699. [PubMed: 17452023]

Marfella CGA, Henninger N, LeBlanc SE, Krishnan N, Garlick DS, Holzman LB, Imbalzano AN. A mutation in the mouse chd2 chromatin remodeling enzyme results in a complex renal phenotype. Kidney Blood Press. Res. 2008; 31:421–432. [PubMed: 19142019]

Marfella CGA, Ohkawa Y, Coles AH, Garlick DS, Jones SN, Imbalzano AN. Mutation of the snf2 family member chd2 affects mouse development and survival. J. Cell. Physiol. 2006; 209:162–171. [PubMed: 16810678]

Matsui D, Sakari M, Sato T, Murayama A, Takada I, Kim M, Takeyama K, Kato S. Transcriptional regulation of the mouse steroid 5alpha-reductase type ii gene by progesterone in brain. Nucleic Acids Res. 2002; 30:1387–1393. [PubMed: 11884637]

McGowan RA, Martin CC. Dna methylation and genome imprinting in the zebrafish, danio rerio: some evolutionary ramifications. Biochem. Cell Biol. 1997; 75:499–506. [PubMed: 9551175]

Mehta V, Abler LL, Keil KP, Schmitz CT, Joshi PS, Vezina CM. Atlas of wnt and r-spondin gene expression in the developing male mouse lower urogenital tract. Dev. Dyn. 2011; 240:2548–2560. [PubMed: 21936019]

Metzger E, Wissmann M, Yin N, Müller JM, Schneider R, Peters AHFM, Günther T, Buettner R, Schüle R. Lsd1 demethylates repressive histone marks to promote androgen-receptor-dependent transcription. Nature. 2005; 437:436–439. [PubMed: 16079795]

Modrich P. Mechanisms and biological effects of mismatch repair. Annu. Rev. Genet. 1991; 25:229–253. [PubMed: 1812808]

Modrich P. Mechanisms in eukaryotic mismatch repair. J. Biol. Chem. 2006; 281:30305–30309. [PubMed: 16905530]

Morgan HD, Dean W, Coker HA, Reik W, Petersen-Mahrt SK. Activation-induced cytidine deaminase deaminates 5-methylcytosine in dna and is expressed in pluripotent tissues: implications for epigenetic reprogramming. J. Biol. Chem. 2004; 279:52353–52360. [PubMed: 15448152]

Muramatsu M, Kinoshita K, Fagarasan S, Yamada S, Shinkai Y, Honjo T. Class switch recombination and hypermutation require activation-induced cytidine deaminase (AID), a potential RNA editing enzyme. Cell. 2000; 102:553–563. [PubMed: 11007474]

Nagarajan P, Onami TM, Rajagopalan S, Kania S, Donnell R, Venkatachalam S. Role of chromodomain helicase dna-binding protein 2 in dna damage response signaling and tumorigenesis. Oncogene. 2009; 28:1053–1062. [PubMed: 19137022]

Ng HH, Zhang Y, Hendrich B, Johnson CA, Turner BM, Erdjument-Bromage H, Tempst P, Reinberg D, Bird A. Mbd2 is a transcriptional repressor belonging to the mecp1 histone deacetylase complex. Nat. Genet. 1999; 23:58–61. [PubMed: 10471499]

Okano M, Bell DW, Haber DA, Li E. Dna methyltransferases dnmt3a and dnmt3b are essential for de novo methylation and mammalian development. Cell. 1999; 99:247–257. [PubMed: 10555141]

Popp C, Dean W, Feng S, Cokus SJ, Andrews S, Pellegrini M, Jacobsen SE, Reik W. Genome-wide erasure of dna methylation in mouse primordial germ cells is affected by aid deficiency. Nature. 2010; 463:1101–1105. [PubMed: 20098412]

Prolla TA, Pang Q, Alani E, Kolodner RD, Liskay RM. MLH1, PMS1, and MSH2 interactions during the initiation of DNA mismatch repair in yeast. Science. 1994; 265:1091–1093. [PubMed: 8066446]

Rai K, Huggins IJ, James SR, Karpf AR, Jones DA, Cairns BR. Dna demethylation in zebrafish involves the coupling of a deaminase, a glycosylase, and gadd45. Cell. 2008; 135:1201–1212. [PubMed: 19109892]

Rajagopalan S, Nepa J, Venkatachalam S. Chromodomain helicase dna-binding protein 2 affects the repair of x-ray and uv-induced dna damage. Environ. Mol. Mutagen. 2012; 53:44–50. [PubMed: 22223433]

Reenan RA, Kolodner RD. Isolation and characterization of two Saccharomyces cerevisiae genes encoding homologs of the bacterial HexA and MutS mismatch repair proteins. Genetics. 1992; 132:963–973. [PubMed: 1459447]

Sebag IA, Gillis MA, Calderone A, Kasneci A, Meilleur M, Haddad R, Noiles W, Patel B, Chalifour LE. Sex hormone control of left ventricle structure/function: mechanistic insights using echocardiography, expression, and DNA methylation analyses in adult mice. Am J Physiol Heart Circ Physiol. 2011; 301:H1706–H1715. [PubMed: 21803942]

Soni A, Bansal A, Singh LC, Mishra AK, Majumdar M, Regina T, Mohanty NK, Saxena S. Gene expression profile and mutational analysis of dna mismatch repair genes in carcinoma prostate in indian population. OMICS. 2011; 15:319–324. [PubMed: 21348638]

Su S-S, Modrich P. Escherichia coli mutS-encoded protein binds to mismatched DNA base pairs. Proc. Natl. Acad. Sci. 1986; 83:5057–5061. [PubMed: 3014530]

Sugimura Y, Cunha GR, Donjacour AA. Morphogenesis of ductal networks in the mouse prostate. Biol. Reprod. 1986; 34:961–971. [PubMed: 3730488]

Tahiliani M, Koh KP, Shen Y, Pastor WA, Bandukwala H, Brudno Y, Agarwal S, Iyer LM, Liu DR, Aravind L, Rao A. Conversion of 5-methylcytosine to 5-hydroxymethylcytosine in mammalian dna by mll partner tet1. Science. 2009; 324:930–935. [PubMed: 19372391]

Takeda H, Chang C. Immunohistochemical and in-situ hybridization analysis of androgen receptor expression during the development of the mouse prostate gland. J. Endocrinol. 1991; 129:83–89. [PubMed: 2030333]

Takeda H, Lasnitzki I, Mizuno T. Change of mosaic pattern by androgens during prostatic bud formation in xtfm/x+ heterozygous female mice. J. Endocrinol. 1987; 114:131–137. [PubMed: 3655602]

Tan L, Shi YG. Tet family proteins and 5-hydroxymethylcytosine in development and disease. Development. 2012; 139:1895–1902. [PubMed: 22569552]

Tang W, Morey LM, Cheung YY, Birch L, Prins GS, Ho S. Neonatal exposure to estradiol/bisphenol a alters promoter methylation and expression of nsbp1 and hpcal1 genes and transcriptional programs of dnmt3a/b and mbd2/4 in the rat prostate gland throughout life. Endocrinology. 2012; 153:42–55. [PubMed: 22109888]

Timms BG, Howdeshell KL, Barton L, Bradley S, Richter CA, vom Saal FS. Estrogenic chemicals in plastic and oral contraceptives disrupt development of the fetal mouse prostate and urethra. Proc. Natl. Acad. Sci. U.S.A. 2005; 102:7014–7019. [PubMed: 15867144]

van Kaam KJAF, Delvoux B, Romano A, D'Hooghe T, Dunselman GAJ, Groothuis PG. Deoxyribonucleic acid methyltransferases and methyl-cpg-binding domain proteins in human endometrium and endometriosis. Fertil. Steril. 2011; 95:1421–1427. [PubMed: 21316665]

Varlet I, Pallard C, Radman M, Moreau J, de Wind N. Cloning and expression of the Xenopus and mouse Msh2 DNA mismatch repair genes. Nucleic Acids Res. 1994; 22:5723–5728. [PubMed: 7838728]

Vezina CM, Allgeier SH, Moore RW, Lin T, Bemis JC, Hardin HA, Gasiewicz TA, Peterson RE. Dioxin causes ventral prostate agenesis by disrupting dorsoventral patterning in developing mouse prostate. Toxicol. Sci. 2008; 106:488–496. [PubMed: 18779384]

Vincent ZL, Farquhar CM, Mitchell MD, Ponnampalam AP. Expression and regulation of dna methyltransferases in human endometrium. Fertil. Steril. 2011; 95:1522–1525. e1. [PubMed: 20970125]

Wagner DG, Gatalica Z, Lynch HT, Kohl S, Johansson SL, Lele SM. Neuroendocrine-type prostatic adenocarcinoma with microsatellite instability in a patient with lynch syndrome. Int. J. Surg. Pathol. 2010; 18:550–553. [PubMed: 20798067]

Walker CL. Epigenomic reprogramming of the developing reproductive tract and disease susceptibility in adulthood. Birth Defects Res. Part A Clin. Mol. Teratol. 2011; 91:666–671. [PubMed: 21656660]

Wang D, Chen Q, Zhang C, Ren F, Li T. Dna hypomethylation of the cox-2 gene promoter is associated with up-regulation of its mrna expression in eutopic endometrium of endometriosis. Eur. J. Med. Res. 2012; 17:12. [PubMed: 22608095]

Wissmann M, Yin N, Müller JM, Greschik H, Fodor BD, Jenuwein T, Vogler C, Schneider R, Günther T, Buettner R, Metzger E, Schüle R. Cooperative demethylation by jmjd2c and lsd1 promotes androgen receptor-dependent gene expression. Nat. Cell Biol. 2007; 9:347–353. [PubMed: 17277772]

Xu N, Kwon S, Abbott DH, Geller DH, Dumesic DA, Azziz R, Guo X, Goodarzi MO. Epigenetic mechanism underlying the development of polycystic ovary syndrome (pcos)-like phenotypes in prenatally androgenized rhesus monkeys. PLoS One. 2011; 6:e27286. [PubMed: 22076147]

Yamagata Y, Asada H, Tamura I, Lee L, Maekawa R, Taniguchi K, Taketani T, Matsuoka A, Tamura H, Sugino N. Dna methyltransferase expression in the human endometrium: down-regulation by progesterone and estrogen. Hum. Reprod. 2009; 24:1126–1132. [PubMed: 19202141]

Ye J, Coulouris G, Zaretskaya I, Cutcutache I, Rozen S, Madden T. Primer-BLAST: A tool to design target-specific primers for polymerase chain reaction. BMC Bioinformatics. 2012; 13:134. [PubMed: 22708584]

Zhang Z, Schwartz S, Wagner L, Miller W. A greedy algorithm for aligning DNA sequences. J. Comput. Biol. 2000; 7:203–214. [PubMed: 10890397]

Zelenko Z, Aghajanova L, Irwin JC, Giudice LC. Nuclear receptor, coregulator signaling, and chromatin remodeling pathways suggest involvement of the epigenome in the steroid hormone response of endometrium and abnormalities in endometriosis. Reprod Sci. 2012; 19:152–162. [PubMed: 22138541]

Zhu B, Zheng Y, Angliker H, Schwarz S, Thiry S, Siegmann M, Jost JP. 5-methylcytosine dna glycosylase activity is also present in the human mbd4 (g/t mismatch glycosylase) and in a related avian sequence. Nucleic Acids Res. 2000a; 28:4157–4165. [PubMed: 11058112]

Zhu B, Zheng Y, Hess D, Angliker H, Schwarz S, Siegmann M, Thiry S, Jost JP. 5-methylcytosine-dna glycosylase activity is present in a cloned g/t mismatch dna glycosylase associated with the chicken embryo dna demethylation complex. Proc. Natl. Acad. Sci. U.S.A. 2000b; 97:5135–5139. [PubMed: 10779566]

Zhu J. Active dna demethylation mediated by dna glycosylases. Annu. Rev. Genet. 2009; 43:143–166. [PubMed: 19659441]

Zong Y, Huang J, Sankarasharma D, Morikawa T, Fukayama M, Epstein JI, Chada KK, Witte ON. Stromal epigenetic dysregulation is sufficient to initiate mouse prostate cancer via paracrine wnt signaling. Proc. Natl. Acad. Sci. U.S.A. 2012; 109:E3395–E3404. [PubMed: 23184966]

Highlights

- DNA methyltransferase mRNAs are present in mouse lower urinary tract and prostate
- DNA demethylation mRNAs are present in mouse lower urinary tract and prostate
- Spatio-temporal expression of these mRNAs changes during prostate development
- Differences in expression are seen between male and female in some of these mRNAs

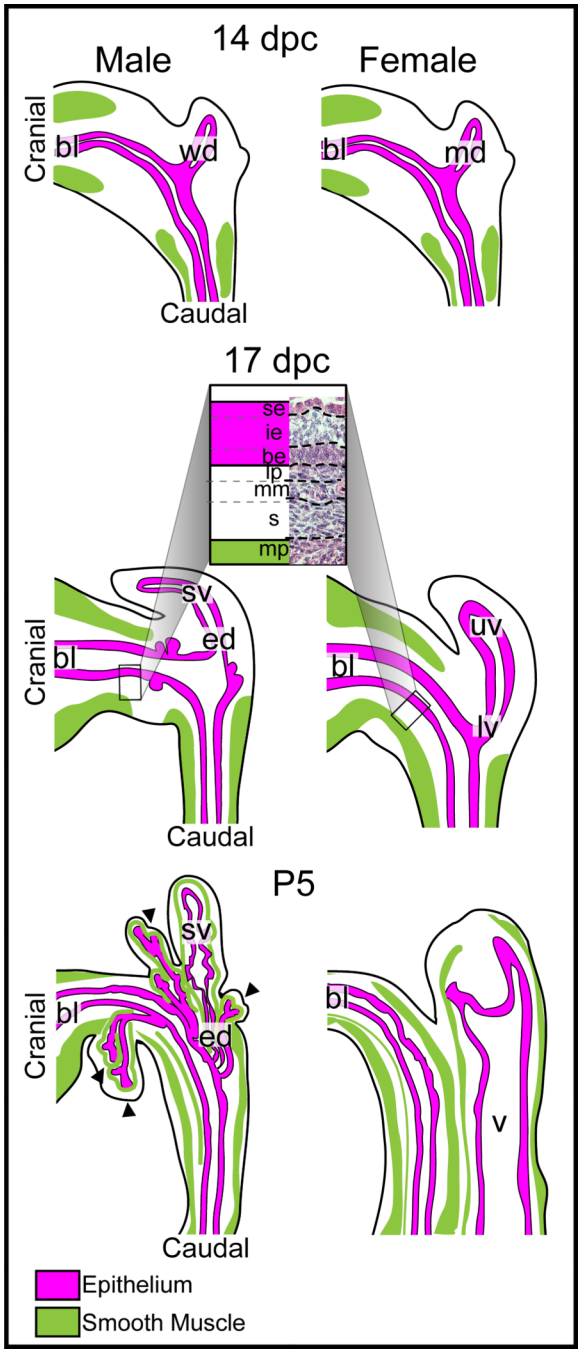

Fig. 1.

Schematic representation of near mid-sagittal 14.5 dpc, 17.5 dpc and P5 male and female mouse LUT. Smooth muscle (muscularis propria) is indicated in green and epithelium in pink. These same tissue compartments were fluorescently labeled to serve as anatomical landmarks in the mapping of mRNA expression patterns in subsequent figures. The inset consists of a schematic representation as well as a 20x hematoxolin and eosin stained 5μm mid-sagittal section of the layers present in the dorsal and ventral pelvic urethra. Three epithelial and four mesenchymal urethral sub-compartments are present at 17.5 dpc as indicated in the inset with the following abbreviations; se, superficial epithelium; ie, intermediate epithelium; be, basal epithelium; lp, lamina propria; mm, muscularis mucosa; s,

submucosa; mp, muscularis propria. Other abbreviations bl, bladder; wd, Wolffian duct; md, Mullerian duct; sv, seminal vesicle; ed, ejaculatory duct; lv, lower vagina; uv, upper vagina. Closed arrowheads indicate prostatic buds.

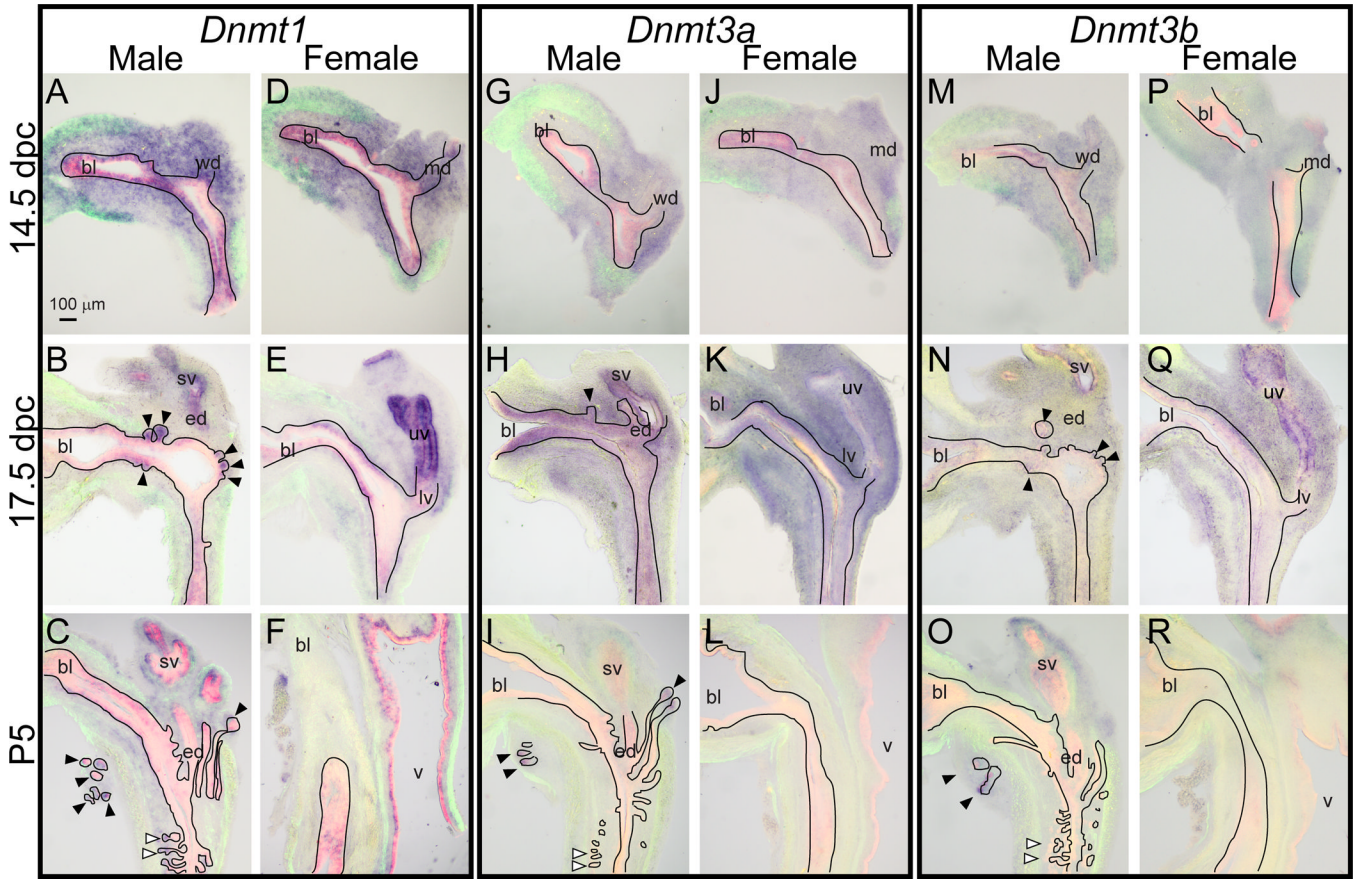

Fig 2.

Dnmt1, Dnmt3a and *Dnmt3b* mRNA expression in developing male and female mouse LUT. ISH was used to visualize mRNA expression (purple) of (A–F) *Dnmt1*, (G–L) *Dnmt3a*, and (M–R) *Dnmt3b* in near midsagittal sections (50μm) of 14.5 dpc, 17.5 dpc and P5 male and female LUTs. Sections were then immunofluorescently stained with antibodies against CDH1 (red) to label all epithelium and ACTA2 (green) to label smooth muscle present in mesenchyme. Results are representative of three litter-independent samples per gender and age. bl, bladder; ed, ejaculatory duct; lv, lower vagina; md, Müllerian duct; sv, seminal vesicle; uv, upper vagina; v, vagina; wd, Wolffian duct. Closed arrowheads indicate prostatic buds; open arrowheads indicate urethral gland buds. A black line separates mesenchyme from epithelium within the pelvic urethra, prostatic buds and urethral gland buds.

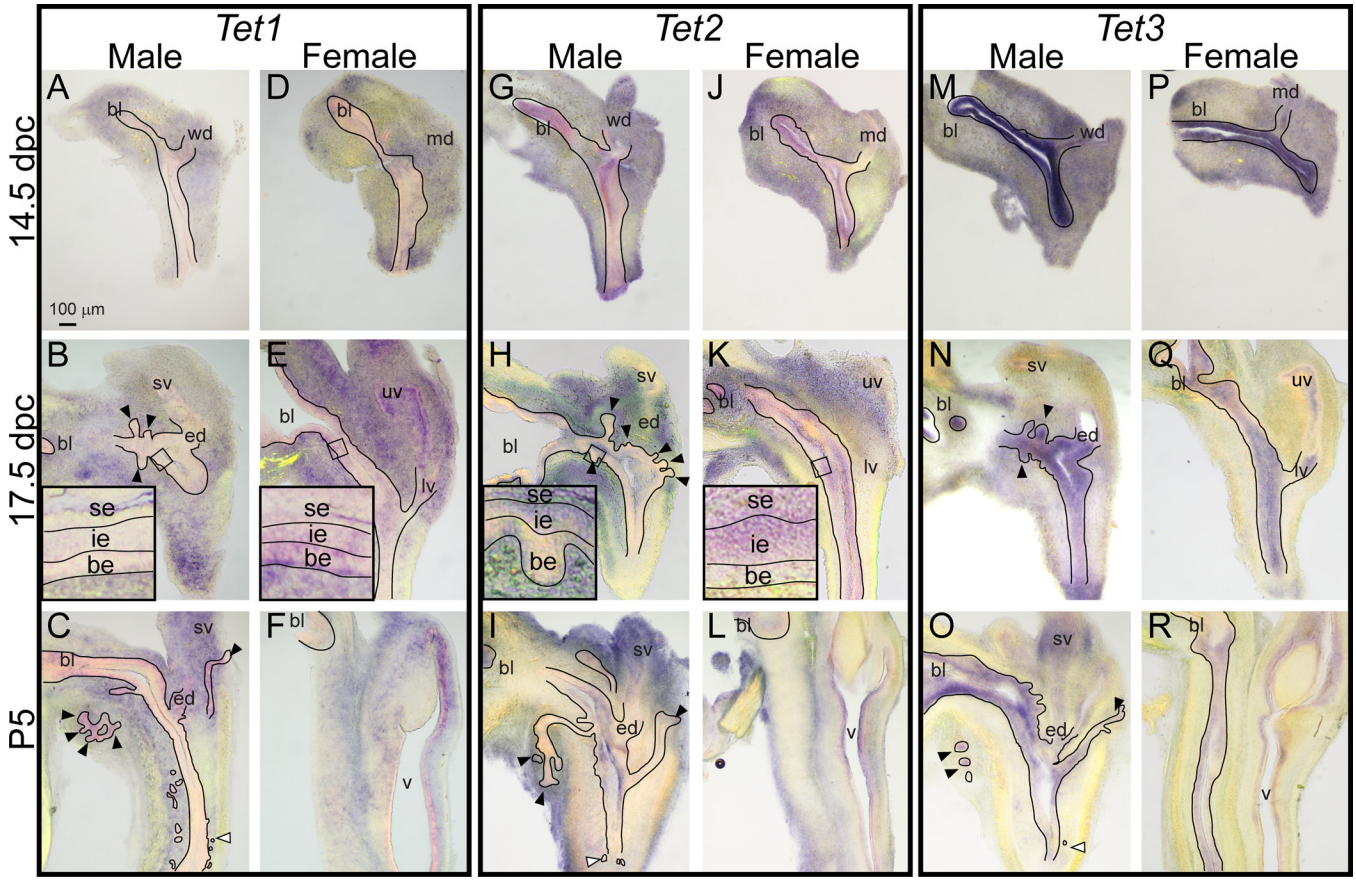

Fig 3.

Tet1, Tet2 and *Tet3* mRNA expression in developing male and female mouse LUT. ISH was used to visualize mRNA expression (purple) of (A–F) *Tet1*, (G–L) *Tet2*, and (M–R) *Tet3* in near midsagittal sections (50μm) of 14.5 dpc, 17.5 dpc and P5 male and female LUTs. Sections were then immunofluorescently stained with antibodies against CDH1 (red) to label all epithelium and ACTA2 (green) to label smooth muscle present in mesenchyme. Results are representative of three litter-independent samples per gender and age. be, basal epithelium; bl, bladder; ed, ejaculatory duct; ie, intermediate epithelium; lv, lower vagina; md, Müllerian duct; se, superficial epithelium; sv, seminal vesicle; uv, upper vagina; v, vagina; wd, Wolffian duct. Closed arrowheads indicate prostatic buds; open arrowheads indicate urethral gland buds. A black line separates mesenchyme from epithelium within the pelvic urethra, prostatic buds and urethral gland buds. Insets are enlarged from the same image in the region indicated by the black box.

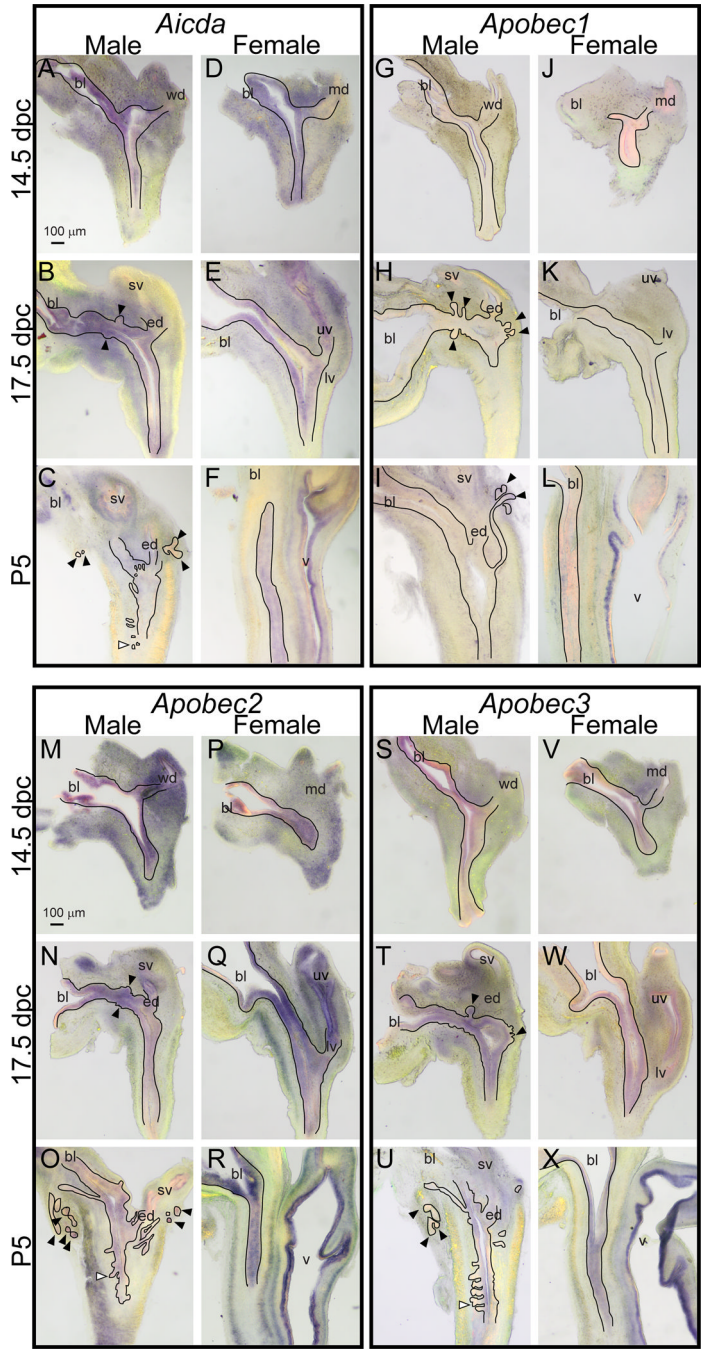

Fig 4.

Aicda, Apobec1, Apobec 2 and *Apobec3* mRNA expression in developing male and female mouse LUT. ISH was used to visualize mRNA expression (purple) of (A–F) *Aicda*, (G–L) *Apobec1*, (M–R) *Apobec2* and (S–X) *Apobec3* in near midsagittal sections (50μm) of 14.5 dpc, 17.5 dpc and P5 male and female LUTs. Sections were then immunofluorescently stained with antibodies against CDH1 (red) to label all epithelium and ACTA2 (green) to label smooth muscle present in mesenchyme. Results are representative of three litter-independent samples per gender and age. bl, bladder; ed, ejaculatory duct; lv, lower vagina; md, Müllerian duct; sv, seminal vesicle; uv, upper vagina; v, vagina; wd, Wolffian duct. Closed arrowheads indicate prostatic buds; open arrowheads indicate urethral gland buds. A

black line separates mesenchyme from epithelium within the pelvic urethra, prostatic buds and urethral gland buds.

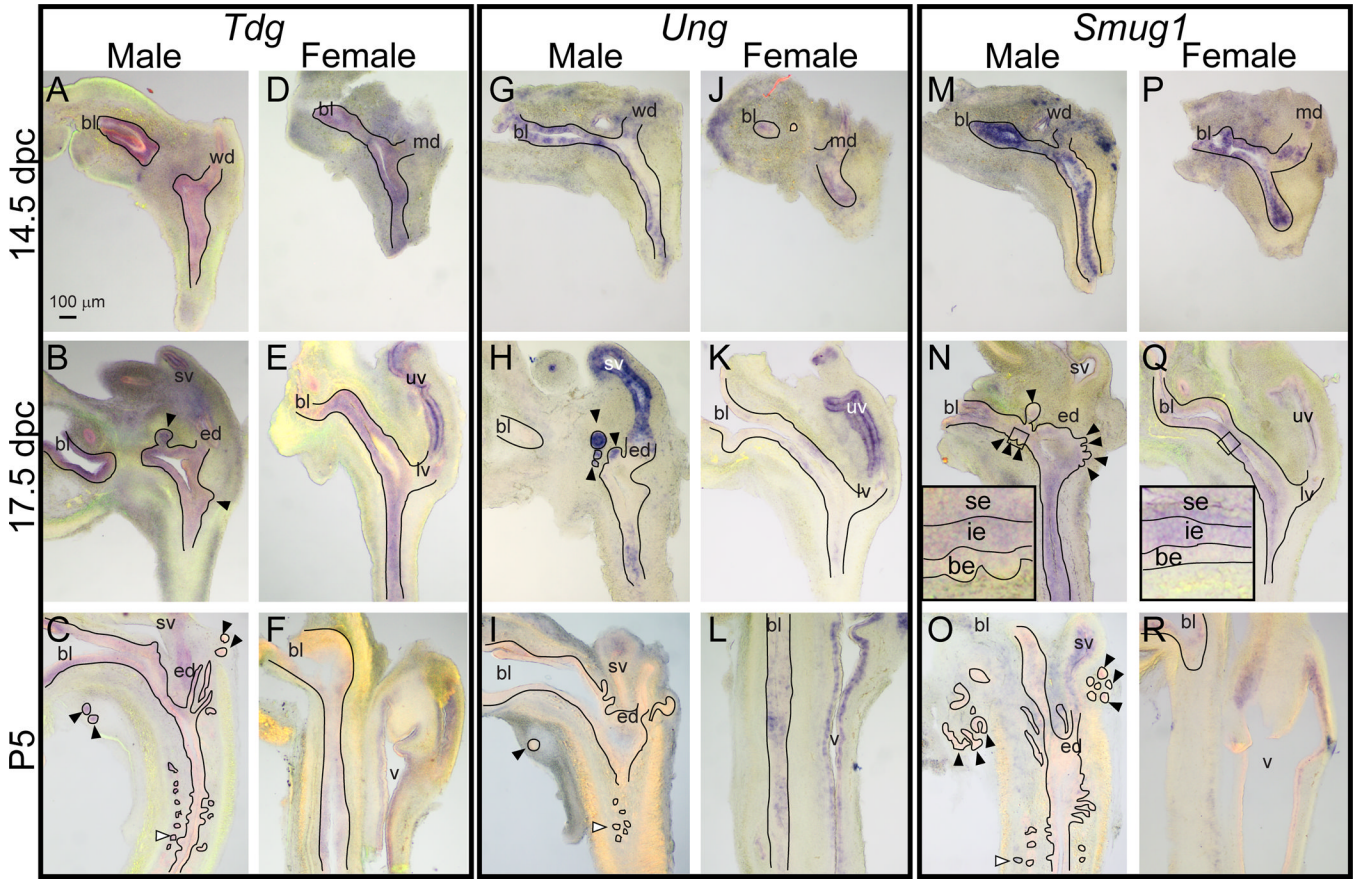

Fig 5.

Tdg, Ung, and *Smug1* mRNA expression in developing male and female mouse LUT. ISH was used to visualize mRNA expression (purple) of (A–F) *Tdg*, (G–L) *Ung*, and (M–R) *Smug1* in near midsagittal sections (50μm) of 14.5 dpc, 17.5 dpc and P5 male and female LUTs. Sections were then immunofluorescently stained with antibodies against CDH1 (red) to label all epithelium and ACTA2 (green) to label smooth muscle present in mesenchyme. Results are representative of three litter-independent samples per gender and age. be, basal epithelium; bl, bladder; ed, ejaculatory duct; ie, intermediate epithelium; lv, lower vagina; md, Müllerian duct; se, superficial epithelium; sv, seminal vesicle; uv, upper vagina; v, vagina; wd, Wolffian duct. Closed arrowheads indicate prostatic buds; open arrowheads indicate urethral gland buds. A black line separates mesenchyme from epithelium within the pelvic urethra, prostatic buds and urethral gland buds. Insets are enlarged from the same image in the region indicated by the black box.

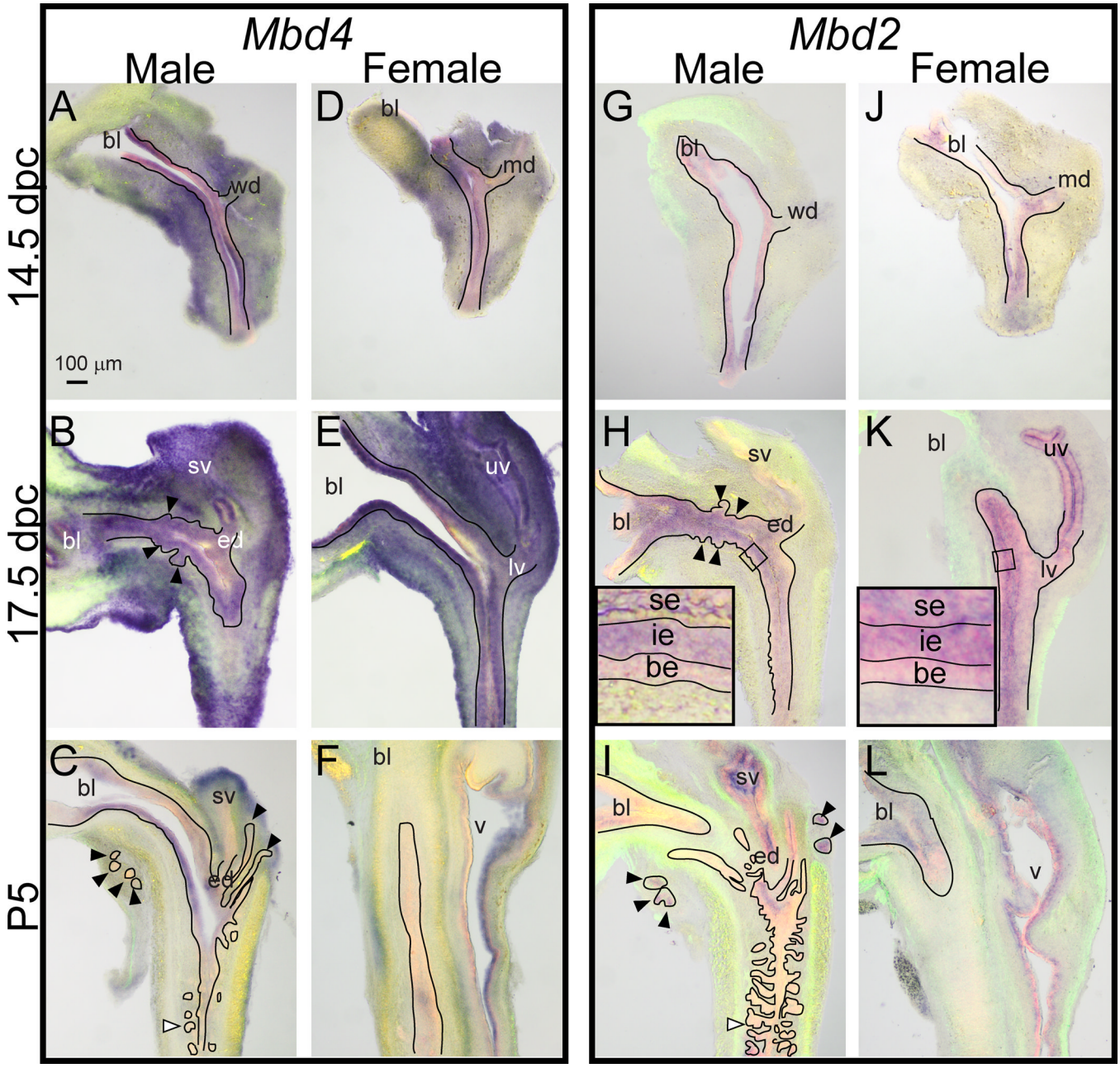

Fig 6.

Mbd4 and *Mbd2* mRNA expression in developing male and female mouse LUT. ISH was used to visualize mRNA expression (purple) of (A–F) *Mbd4*, and (G–L) *Mbd2* in near midsagittal sections (50μm) of 14.5 dpc, 17.5 dpc and P5 male and female LUTs. Sections were then immunofluorescently stained with antibodies against CDH1 (red) to label all epithelium and ACTA2 (green) to label smooth muscle present in mesenchyme. Results are representative of three litter-independent samples per gender and age. be, basal epithelium; bl, bladder; ed, ejaculatory duct; ie, intermediate epithelium; lv, lower vagina; md, Müllerian duct; se, superficial epithelium; sv, seminal vesicle; uv, upper vagina; v, vagina; wd, Wolffian duct. Closed arrowheads indicate prostatic buds; open arrowheads indicate urethral gland buds. A black line separates mesenchyme from epithelium within the pelvic urethra,

prostatic buds and urethral gland buds. Insets are enlarged from the same image in the region indicated by the black box.

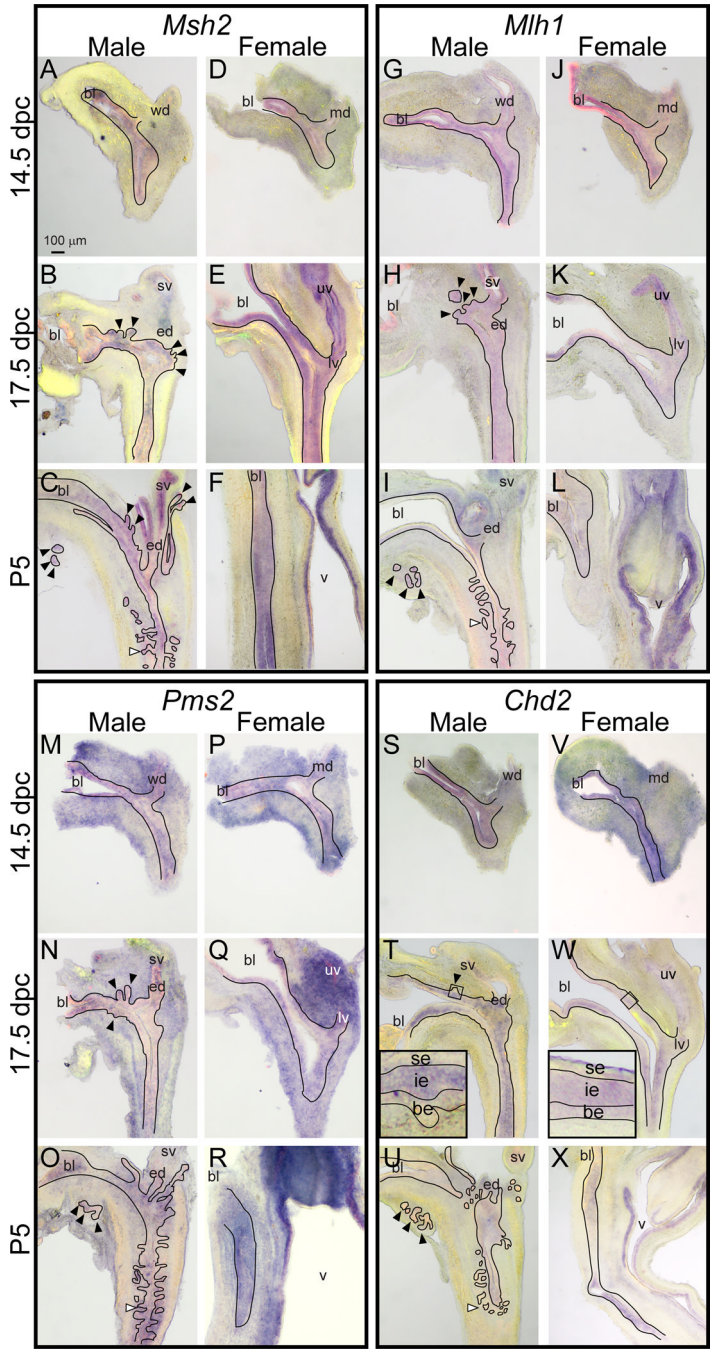

Fig 7.

Msh2, Mlh1, Pms2 and *Chd2* mRNA expression in developing male and female mouse LUT. ISH was used to visualize mRNA expression (purple) of (A–F) *Msh2*, (G–L) *Mlh1*, (M–R) *Pms2* and (S–X) *Chd2* in near midsagittal sections (50μm) of 14.5 dpc, 17.5 dpc and P5 male and female LUTs. Sections were then immunofluorescently stained with antibodies against CDH1 (red) to label all epithelium and ACTA2 (green) to label smooth muscle present in mesenchyme. Results are representative of three litter-independent samples per gender and age. be, basal epithelium; bl, bladder; ed, ejaculatory duct; ie, intermediate epithelium; lv, lower vagina; md, Müllerian duct; se, superficial epithelium; sv, seminal vesicle; uv, upper vagina; v, vagina; wd, Wolffian duct. Closed arrowheads indicate

prostatic buds; open arrowheads indicate urethral gland buds. A black line separates mesenchyme from epithelium within the pelvic urethra, prostatic buds and urethral gland buds. Insets are enlarged from the same image in the region indicated by the black box.

Table 1

PCR primers used to synthesize digoxygenin-labeled riboprobes.

Symbol	Gene Name	Genbank number (and probe position)	Left Primer Sequence (5' → 3')	Right Primer sequence (5' → 3') T7 binding site is in bold text
Aicda	activation-induced cytidine deaminase	NM_009645.2 (1447–2184)	AGATCGCGTCCCTTA AACATC	CGATGT**TAATACGACTCACTATAGGG**TGG GAGTCTATGTTGGTTTCC
Apobec1	apolipoprotein B mRNA editing enzyme, catalytic polypeptide 1	NM_001134391.1 (1308–2027)	GAGGTGTCATTCATG GGTAGG	CGATGT**TAATACGACTCACTATAGGG**CAG AACGGCTAACAGATGGAG
Apobec2	apolipoprotein B mRNA editing enzyme, catalytic polypeptide 2	NM_009694.3 (549–1085)	AACCTTCGTCTGCTC ATTCTG	CGATGT**TAATACGACTCACTATAGGG**AGA GGCAATAAGACCCTCCAC
Apobec3	apolipoprotein B mRNA editing enzyme, catalytic polypeptide 3	NM_001160415.1 (1353–2020)	TGGTGAATGACTTTG GAAACC	CGATGT **T AATACGACTCACTATAGGG**TCAT TGTATAGCCCAGGATGTG
Chd2	chromodomain helicase DNA binding protein 2	NM_001081345.2 (7966–8748)	GATTTGCTGAGCTCT TGGATG	CGATGT**TAATACGACTCACTATAGGG**TGG GTTTGTTTGGTCTGTAGG
Dnmt1	DNA methyltransferase (cytosine-5) 1	NM_010066.3 (4559–5147)	GCAATTCAGCACCCT CATC	CGATGT**TAATACGACTCACTATAGGG**AAAC CAAACCAAACCAAACC
Dnmt3a	DNA methyltransferase 3A	NM_007872.4 (8526–9097)	TACAGCTTGCTGCAC TCTCC	CGATGT**TAATACGACTCACTATAGGG**TCCA TAAGTCCCTGCTGGTC
Dnmt3b	DNA methyltransferase 3B	NM_001003961.3 (1324–1943)	AGGAAGGCCATGTA CCACAC	CGATGT**TAATACGACTCACTATAGGG**AGC ACCTCCAGACACTCCAC
Mbd2	methyl-CpG binding domain protein 2	NM_010773.2 (1244–1820)	GGAAGAGCGAGTCC AACAAG	CGATGT**TAATACGACTCACTATAGGG**TCTT TACAGTGATGATGGAAGAATG
Mbd4	methyl-CpG binding domain protein 4	NM_010774.2 (2401–3260)	AGGTTGGCCTCTTAC CTTCAC	CGATGT**TAATACGACTCACTATAGGG**CAAA GCTGCCTTCACACTCTC
Mlh1	mutL homolog 1	NM_026810.2 (1514–2285)	ATCGGGAGGACTCT GATGTG	CGATGT**TAATACGACTCACTATAGGG**GTA GGAGGTGTGAGCGGAAG
Msh2	mutS homolog 2	NM_008628.2 (2245–2912)	CTCAGGTCAGCAACC AAAGAC	CGATGT**TAATACGACTCACTATAGGG**AGC ACTACCCAGAACAGCAC
Pms2	postmeiotic segregation increased 2	NM_008886.2 (2443–2961)	GCCCTCACGAGTCA GACAG	CGATGT**TAATACGACTCACTATAGGG**CACA AAGTCAAATTGCAGAACAG
Smug1	single-strand selective monofunctional uracil DNA glycosylase	NM_027885.3 (2578–3430)	CCTTTGCCTATAACC CTGCTC	CGATGT**TAATACGACTCACTATAGGG**CACA AACCAGCACCAAATACC
Tdg	thymine DNA glycosylase	NM_011561.2 (736–1443)	CATGGATGACCACAC CTTACC	CGATGT**TAATACGACTCACTATAGGG**TAAG CGTGGCTCTCTTCTTCC
Tet1	tet methylcytosine dioxygenase 1	NM_027384.1 (11307–11807)	TTGAGGGACTGAGA CAGGATG	CGATGT**TAATACGACTCACTATAGGG**TGGT AGCTCATCACCAAGGAC
Tet2	tet methylcytosine dioxygenase 2	NM_001040400.2 (6392–7144)	TGGTTCTCTTATTGG CTGAGG	CGATGT**TAATACGACTCACTATAGGG**TATC CATTCAGCTTCGGTTTG
Tet3	tet methylcytosine dioxygenase 3	NM_183138.2 (9811–10550)	TGTCCATCTCATCGA GCTTTC	CGATGT**TAATACGACTCACTATAGGG**CCTA CCATTCATCCATCAACC
Ung	uracil DNA glycosylase	NM_001040691.1 (770–1313)	GCTGAATCAGAACCT GAGTGG	CGATGT**TAATACGACTCACTATAGGG**AAAC TGCTGGTCCAAAGGTG